

1. Preparation of Standard Curves for Organic Dye Solutions

To establish the relationship between absorbance and the concentration of a methyl orange solution, a standard curve was prepared to facilitate subsequent adsorption experiments. Different concentrations of methyl orange solutions were obtained by diluting a 2000 mg/L stock solution. Standard solutions with concentrations of 10 mg/L, 20 mg/L, 30 mg/L, 40 mg/L, and 50 mg/L were prepared via serial dilution. The maximum absorption wavelength of the methyl orange solution was determined using a UV–Vis absorption spectrum and set as the detection wavelength. The absorbance (Abs) of each concentration gradient was measured with a UV–Vis spectrophotometer. The data were plotted with concentration on the x-axis and absorbance on the y-axis to generate the standard curve for methyl orange. This curve enables the determination of unknown concentrations by measuring absorbance and referencing the curve and equation. Standard curves for other organic dyes, such as Rhodamine B, methylene blue, methyl blue, and Congo red, were prepared using the same procedure as for methyl orange.

UV–Vis absorption spectra tests were conducted for different gradient concentrations of each organic dye, and the data were plotted to obtain the standard curve for methyl orange, as shown in Figure. S1. The maximum absorption wavelengths for methyl orange, Rhodamine B, methylene blue, methyl blue, and Congo red were found to be 464 nm, 554 nm, 664 nm, 498 nm, and 595 nm, respectively. The fitting equations and coefficients of determination (R^2) for Rhodamine B, methylene blue, methyl blue, and Congo red are as follows:

$$\text{Rhodamine B: } y = 0.1216x + 0.0384 (R^2 = 0.9986) \quad (\text{S1})$$

$$\text{Methylene blue: } y = 0.1888x + 0.1024 (R^2 = 0.9987) \quad (\text{S2})$$

$$\text{Methyl blue: } y = 0.0248x - 0.0065 (R^2 = 0.9982) \quad (\text{S3})$$

$$\text{Congo red: } y = 0.0233x + 0.0022 (R^2 = 1) \quad (\text{S4})$$

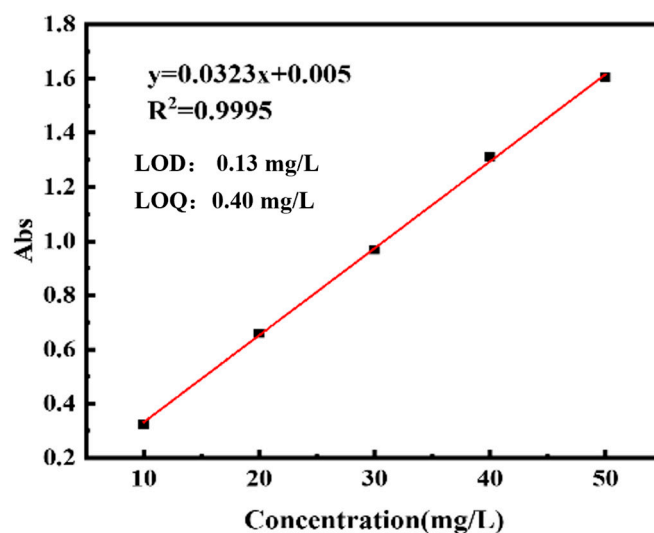


Figure S1. Standard curve of methyl orange.

The BET specific surface area was determined using the multipoint BET method by fitting the linear region of the adsorption isotherm at relative pressures (P/P_0) of 0.05–0.35 based on the BET equation. The total pore volume was calculated from the amount adsorbed at P/P_0 close to 1.0. The average pore diameter was estimated using $4V/A$, derived from the cylindrical pore model.

2. Effect of the PEI and CC Ratio on Methyl Orange Adsorption (Optimization of Preparation Conditions)

Samples of 2 mg of CZ-550 and CZ@PEI/CC- x ($x = 1-8$) materials, synthesized with different PEI-to-CC mass ratios, were placed into conical flasks. Subsequently, 20 mL of a 60 mg/L methyl orange solution was added to each flask. The flasks were sealed with plastic wrap and incubated in a constant-temperature shaker set at 298.15 K and 140 rpm for a predetermined duration. Every 40 minutes, 1.5 mL of the supernatant was extracted using a syringe, filtered through a 0.22 μm microporous membrane, and analyzed with a UV-Vis spectrophotometer to measure absorbance. The corresponding concentration and removal rate were then calculated.

Similarly, samples of 2 mg of CZ-550 and CZ@PEI/CC- x ($x = 5-8$) materials, prepared with various PEI-to-CC synthesis ratios, were placed into conical flasks with 20 mL of 60 mg/L methyl orange solution. Absorbance was recorded every 10 minutes, while the other procedures remained consistent with the steps outlined above.

3. SEM of CZ@PEI/CC- x

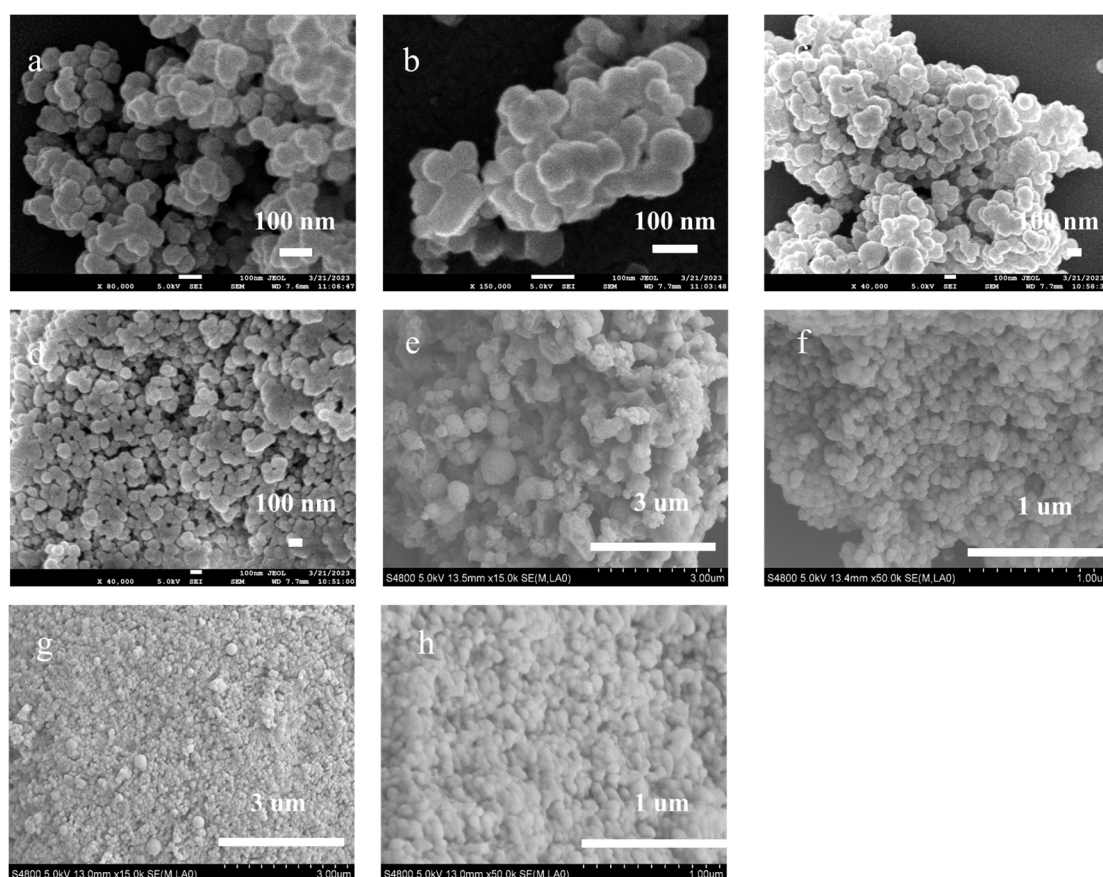


Figure S2. The SEM images of (a) CZ@PEI/CC-1, (b) CZ@PEI/CC-2, (c) CZ@PEI/CC-3, (d) CZ@PEI/CC-4, (e) CZ@PEI/CC-5, (f) CZ@PEI/CC-6, (g) CZ@PEI/CC-7 and (h) CZ@PEI/CC-8.

4.1. Stability Tests

4.2. Water Stability Test

To evaluate water stability, CZ@PEI/CC-7 was dispersed in deionized water to prepare a suspension with an adsorbent concentration of 100 mg/L. An aliquot (20 mL) of the suspension was transferred into an Erlenmeyer flask and shaken at 289.15 K and 140 rpm for 1, 2, 4, and 7 days. After the designated time, the solid was recovered by centrifugation at 6000 rpm for 5 min, dried at 60 $^{\circ}\text{C}$, and analyzed by X-ray diffraction (XRD) to examine possible changes in crystalline structure.

4.3. Acid and Alkali Stability Test

Aqueous solutions with different pH values were prepared by adjusting deionized water using 0.1 mol/L HCl and 0.1 mol/L NaOH. For each pH condition, 20 mL of the pH-adjusted solution was placed in an Erlenmeyer flask, and CZ@PEI/CC-7 was added to obtain a suspension with an adsorbent concentration of 100 mg/L (i.e., 2 mg in 20 mL). The suspension was shaken at 298.15 K and 140 rpm for 24 h. The mixture was then centrifuged at 6000 rpm for 5 min to separate the solid and liquid phases. The Zn^{2+} concentration in the supernatant was determined by inductively coupled plasma optical emission spectrometry (ICP-OES) to quantify Zn^{2+} leaching and thereby assess the acid and alkali stability of the material.

5. Adsorption Characteristics of Methyl Orange on CZ@PEI/CC-7

The adsorption performance toward methyl orange (MO) was investigated under various influencing factors, including adsorbent dosage, solution pH, initial MO concentration, contact time, and temperature.

5.1. Effect of adsorbent dosage

Different amounts of CZ@PEI/CC-7 (1–6 mg) were placed in Erlenmeyer flasks, followed by the addition of 20 mL of MO solution (100 mg/L). The suspensions were sonicated for 1 min, sealed with plastic film, and then shaken in a thermostatic shaking incubator at 298.15 K and 140 rpm for 10 min. After adsorption, 1.5 mL of the supernatant was withdrawn, filtered through a 0.22 μm membrane, and analyzed using a UV–Vis spectrophotometer. The residual MO concentration was determined from the calibration curve, and the removal efficiency was calculated accordingly.

5.2. Effect of solution pH

A 100 mg/L MO solution was prepared by diluting a 2000 mg/L MO stock solution. The pH was adjusted to 2, 4, 6, 8, 10, and 11 using freshly prepared 0.1 mol/L HCl and 0.1 mol/L NaOH. For each pH condition, 20 mL of the pH-adjusted MO solution was transferred into an Erlenmeyer flask, and 3 mg of CZ@PEI/CC-7 was added. Adsorption was performed under the same shaking conditions as above, and samples were collected after 20 min for UV–Vis analysis.

5.3. Effect of initial MO concentration

MO solutions with different initial concentrations (200, 300, 400, 500, 600, 700, 800, 1000, and 1200 mg/L) were prepared by diluting the 2000 mg/L stock solution. For each concentration, 20 mL of MO solution was placed in an Erlenmeyer flask, and 3 mg of CZ@PEI/CC-7 was added. The mixtures were shaken under the same conditions for 24 h to reach equilibrium. After filtration (0.22 μm), the residual MO concentration was measured by UV–Vis.

5.4. Effect of contact time and temperature

To evaluate the effects of contact time and temperature, adsorption experiments were conducted at 298.15, 300.15, 303.15, and 308.15 K. Briefly, 20 mL of MO solution (100 mg/L) was added into an Erlenmeyer flask, followed by 3 mg of CZ@PEI/CC-7. The mixture was shaken at 140 rpm, and aliquots were collected at predetermined time intervals (every 40 min), filtered (0.22 μm), and analyzed by UV–Vis to determine MO concentration.

6. Adsorption Models

6.1. Adsorption kinetics

An amount of 3 mg of CZ@PEI/CC-7 was added to Erlenmeyer flasks containing 20 mL of MO solution (330, 350, 370, 400 mg/L). The mixtures were sonicated for 27s, sealed, and shaken at 298.15 K and 140 rpm. At predetermined time intervals (every 40 min), 0.5 mL of the suspension was withdrawn, filtered through a 0.22 μm membrane, and analyzed by UV–Vis. The adsorption capacity was calculated from the concentration change.

6.2. Adsorption isotherms

For isotherm experiments, 3 mg of CZ@PEI/CC-7 was added to Erlenmeyer flasks containing 20 mL of MO solutions with different initial concentrations. After sonication for 27s, the flasks were sealed and shaken at 140 rpm for 24 h at 298.15, 303.15, and 308.15 K. After equilibrium, the samples were filtered (0.22 μm), and the residual MO concentration was determined by UV–Vis to calculate equilibrium adsorption capacities.

6.3. Thermodynamic analysis

Thermodynamic parameters for MO adsorption on CZ@PEI/CC-7 were evaluated using adsorption data obtained at 298.15, 303.15, and 303.15 K. The standard entropy change (ΔS°) and standard enthalpy change (ΔH°) were derived from the slope and intercept of the linear plot of $\ln K^\circ$ versus $1/T$. The Gibbs free energy change (ΔG°) was subsequently calculated according to the relevant thermodynamic equations.

7. Selective Adsorption and Competitive Adsorption in Binary Systems

7.1. Selective Adsorption Experiments

To compare the adsorption behavior of CZ@PEI/CC-7 toward different dyes and further examine adsorption selectivity, additional anionic and cationic dyes were tested. Methylene blue, Rhodamine B, methyl blue, and Congo red solutions (100 mg/L) were prepared. For each dye, 20 mL of dye solution was placed in an Erlenmeyer flask and 3 mg of CZ@PEI/CC-7 was added. The mixture was sonicated for 27s, sealed, and shaken at 298.15 K and 140 rpm for 40 min. After filtration (0.22 μ m), the dye concentration was determined by UV–Vis, and the adsorption performance was calculated.

7.2. Cyclic Adsorption (Reusability) Experiments

To evaluate the reusability of the adsorbent, adsorption–desorption cycling experiments were performed. Briefly, 3 mg of CZ@PEI/CC-7 was placed in a 50 mL centrifuge tube, and 20 mL of MO solution (100 mg/L) was added. The suspension was sonicated for 27s, sealed, and shaken at 298.15 K and 140 rpm for 40 min. After adsorption, the mixture was centrifuged at 6000 rpm for 5 min to separate the solid and liquid phases. The supernatant (1.5 mL) was filtered (0.22 μ m) and analyzed by UV–Vis to determine the residual MO concentration and adsorption capacity. For regeneration, the supernatant was decanted, and 20 mL of anhydrous ethanol was added to the sedimented adsorbent. The mixture was agitated on a vortex mixer for 20 min to desorb MO, followed by centrifugation at 6000 rpm for 5 min. The supernatant was discarded, and the ethanol desorption step was repeated once to ensure more complete desorption. The final solid was dried at 60 °C for 4 h and reused in the next adsorption cycle. A total of six adsorption–desorption cycles were conducted to assess cyclic adsorption performance.

Table S1. Comparison with other carbon-based materials.

Adsorbent	Material category	Maximum MO adsorption capacity (mg/ g)	Main takeaway	References
rGO-based aerogel	Functionalized reduced graphene oxide aerogel	542.6	High-capacity carbon framework where surface chemistry and diffusion jointly matter	[29]
ZnO@DPS-AC	ZnO loaded activated carbon composite	226.81	Carbon-based support plus inorganic component improves performance	[30]
Activated carbon	Commercial AC	129.3	Typical AC shows moderate capacity and strong temperature dependence	[31]
CZ-550	Carbonized ZIF-8 derived carbon	1100	High adsorption capacity	[28]
CZ@PEI/CC-7	PEI and CC crosslinked carbonized ZIF-8 derived carbon	3150	Ultra-high capacity and excellent stability	This work

Table S2. Key advantages of CZ-550 reported in the literature [28].

Advantage	Evidence in the literature	Key metric / takeaway
High surface area with hierarchical porosity	N ₂ adsorption–desorption indicate predominantly microporous features with the presence of meso-/macropores	BET surface area: 1231.7 m ² ·g ⁻¹
Strongly positive surface charge	A positive zeta potential is reported for CZ-550	Zeta potential: +24 mV
High MO capacity over a wide pH window	The pH applicability and the saturated capacity for MO adsorption	pH 3–13; q _{max} ≈ 1100 mg·g ⁻¹
Combined physisorption–chemisorption nature		Pseudo-second-order kinetics; multiple isotherm models applicable; mixed physical/chemical adsorption

Table S3. Parameters of pseudo-first-order and pseudo-second-order kinetic models for methyl orange adsorption on CZ@PEI/CC-7.

Model	Parameter	330 mg/L	350 mg/L	370 mg/L	400 mg/L
Pseudo-First-Order Kinetic Model	q_{exp}	2198	2323	2478	2603
	q_{cal}	1660	1309	950.5	740.1
	k_1	0.02811	0.01744	0.01270	0.00813
	R^2	0.9632	0.9388	0.9892	0.9815
Pseudo-Second-Order Kinetic Model	q_{cal}	2277.9	2392.3	2570.7	2673.8
	k_2	4.39×10 ⁻⁴	4.18×10 ⁻⁴	3.89×10 ⁻⁴	3.74×10 ⁻⁴
	R^2	0.9999	0.9999	0.9999	0.9999

Table S4. Parameters of the Intraparticle Diffusion and Elovich Kinetic Models for methyl orange adsorption on CZ@PEI/CC-7.

Model	Parameter	330 mg/L	350 mg/L	370 mg/L	400 mg/L
The Intraparticle Diffusion Kinetic Model	K_{d1}	59.84	62.08	64.60	76.08
	C	1478.5	1490.6	1553.3	1491.8
	R^2	0.9899	0.9494	0.9900	0.9797
	K_{d2}	21.64	14.34	21.60	24.76
	C	1885.1	2061.9	2087.8	2114.8
	R^2	0.9788	0.9986	0.9923	0.9979
	K_{d3}	1.27	2.35	7.04	5.39
	C	2176.2	2275.7	2336.0	2461.6
	R^2	0.9994	0.9997	0.9101	0.9548
	α	149019.6	102173.7	22654.2	283614.2
Elovich Kinetic Model	β	0.00552	0.00517	0.00415	0.00678
	R^2	0.9424	0.9193	0.9747	0.9505

Table S5. Parameters of three isotherm models for methyl orange adsorption on CZ@PEI/CC-7.

Model	Parameter	298.15 K	300.15 K	303.15 K
Langmuir	$q_m(\text{mg/g})$	3023.8	2959.9	2998.4
	$K_L(\text{L/mg})$	0.260	1.544	3.291
	R_L	7.63×10^{-3}	1.29×10^{-3}	6.10×10^{-4}
	R^2	0.9884	0.8677	0.8462
Freundlich	K_F	1894.6	2418.8	2555.1
	$1/n$	0.0997	0.0525	0.0473
	R^2	0.9884	0.9939	0.9938
	A_T	608	1.30×10^{-7}	1.70×10^{-8}
Temkin	$B_T(\text{J/mol})$	271.2	146.2	134.2
	R^2	0.9913	0.9882	0.9927